International Journal of Mechanical, Industrial and Aerospace Sciences
ISSN: 2517-9950
Vol:4, No:2, 2010

CFD Modeling of Reduction in NO_X Emission Using HiTAC Technique

Abbas Khoshhal, Masoud Rahimi, Sayed Reza Shabanian, and Ammar Abdulaziz Alsairafi

***Abstract*—**In the present study, the rate of NOx emission in a combustion chamber working in conventional combustion and High Temperature Air Combustion (HiTAC) system are examined using CFD modeling. The effect of peak temperature, combustion air temperature and oxygen concentration on NOx emission rate was undertaken. Results show that in a fixed oxygen concentration, increasing the preheated air temperature will increase the peak temperature and NOx emission rate. In addition, it was observed that the reduction of the oxygen concentration in the fixed preheated air temperature decreases the peak temperature and NOx emission rate. On the other hand, the results show that increase of preheated air temperature at various oxygen concentrations increases the NOx emission rate. However, the rate of increase in HiTAC conditions is quite lower than the conventional combustion. The modeling results show that the NOx emission rate in HiTAC combustion is 133% less than that of the conventional combustion.

***Keywords*—**CFD Modeling, HiTAC, NOx, Combustion.

I. Introduction

DUE to increasing energy demand and dwindling clean fossil fuel reserves on the one hand and due to concern over environmental pollution and global warming due to the greenhouse effect, there is an urgent need for advanced energy systems which deliver efficient power with little environmental cost. High Temperature Air Combustion (HiTAC) which was developed by Tanaka and Hasegawa [1] is one of the most promising combustion techniques that provide solution for energy saving, energy efficiency and pollution formation and emission.

Emission of NOx is now known to be responsible for the destruction of ozone layer in the upper atmosphere. NOx (primarily NO) involves the complicated reaction mechanisms, which result in accelerating the ozone depletion in the oxygen cycle on earth. Therefore, combustion engineers have focused their attention to develop various strategies to reduce NOx emission and improve the combustion process. HiTAC is one of the most advanced techniques because of low levels of NOx formation and emission [2-5].

The principal feature of HiTAC is combustion at extremely diluted oxygen concentration levels with dilution being done either by nitrogen or by carbon dioxide. Due to the low oxygen concentration, the fuel-oxidant mixture is not flammable at near-ambient temperatures. To provide stable combustion, the air is preheated to high temperatures. Thus, in normal combustion, the temperature of the preheated air is kept well below the autoignition temperature of the fuel. In contrast, in HiTAC, the minimum temperature of the preheat air is the autoignition temperature. The oxidant (which is highly diluted with nitrogen or carbon dioxide to about 3 to 5% by weight of oxygen as opposed to 23% in normal combustion) is fed as a separate jet and not as a co-axial jet as in the case of a conventional burner. These features allow strong mixing of the fuel and the oxidant separately with the hot burnt gases within the furnace thus forming a lean combustible mixture over a large volume of the combustor. As a consequence, the heat release associated with combustion takes place over a considerably larger volume and the maximum gas temperature is significantly lower than the adiabatic flame temperature. Reduction of the peak temperature leads to low NOx formation rates as thermal NOx formation [6]. Thus, the principal features of HiTAC, as far as NOx reduction are concerned, are low oxygen concentrations, lean fuel-to-air mixtures and large volume of combustion resulting in low peak temperatures.

Gupta and Li [7] observed that NOx emission at an air pre-heat temperature of 1150°C decreased from 2800 ppm at 21% O_2 to 40 ppm at 2% O_2.

Hasigawa et al. [8] presented NOx emission as a function of oxygen concentration in air and air pre-heat temperature.

The numerical calculation of the combustion process is a three-dimensional problem that involves turbulence, combustion, radiation in addition to NOx modeling. Complex three-dimensional models for equipment design and operational changes are usually based on computational fluid dynamics (CFD). CFD models are founded on fundamental physical principles and can thus predict fluid flow and heat transfer properties within combustion chamber and under specific operational conditions. Submodels such as combustion, turbulence, and NOx formation can be added as subroutines. The mechanisms of NOx formation and correlations can be captured by mathematical models, and their dependence on furnace operating conditions and fuel composition.

Kokkinos et al. [9] applied some techniques for reducing NOx emissions from tangentially fired boilers. They applied staged combustion along the combustors front and rear walls through rerouting the location of some fuel and oxidant feed ports. They used a numerical approach to optimize the design to minimize NOx emissions and reported a decrease of 50% from baseline levels.

Determination of NOx emissions from strong swirling confined flames with an integrated CFD-based procedure was conducted by Frassoldati et al. [10]. The model used very detailed and comprehensive reaction schemes on the basis of the results obtained from CFD computations. The procedure was validated in the case of high swirled con-fined natural gas diffusion flames.

In the present research, the rate of NOx emission in the combustion chamber under conditions known as conventional combustion and HiTAC was examined using CFD modeling. The main aim of this work was to reduce the NOx emission and formation in the combustion systems. The NOx emission in the combustion chamber is depended on peak temperature. The peak temperature, in turn, is depended on preheat air temperature and oxygen concentration. In this line, the study of above mentioned parameters' effects on each other and on NOx emission' was conducted.

II. Theory

Industrial combustion simulations typically involve the solution of the turbulent flows with heat transfer, species transport and chemical reactions. It is common to use the Reynolds-averaged from of the governing equation in conjunction with a suitable turbulence model. Addition equations, such as for radative transport or for specialized combustion models, are also used. The 3-D Reynolds Averaged Navier–Stokes (RANS) equations together with standard $k-\varepsilon$ turbulence model are solved in commercial CFD software package Fluent 6.2 [11]. The conservation equations are given as follows.

A. Continuity Equation

The Reynolds-averaged mixture continuity equation for the gas phase is:

$$\frac{\partial}{\partial t}(\rho)+\nabla\cdot(\rho V)=S_m \tag{1}$$

Where t is time, ρ is the Reynolds-averaged mixture density, V is the Reynolds-averaged velocity vector and S_m represents external mass source.

B. Momentum Equation

The Reynolds-averaged gas-phase momentum equation is given by:

$$\frac{\partial}{\partial t}(\rho V)+\nabla\cdot(\rho VV)=\nabla\cdot((\mu+\mu_t)\nabla V)+F \tag{2}$$

Where μ_t is the turbulent viscosity, obtained from a turbulence model F contains those parts of the stress term not shown explicitly as well as other momentum sources, such as drag from the dispersed phase.

C. Energy Equation

Heat transfer is governed by the energy conservation equation:

$$\frac{\partial}{\partial t}(\rho E)+\nabla\cdot(\rho VE)=\nabla\cdot((k+k_t)\nabla T)+\nabla\cdot(\tau\cdot V)-\nabla\cdot(pV)+S_r+S_h \tag{3}$$

Where k is the thermal conductivity, k_t is the turbulent thermal conductivity resulting from the turbulence model, τ is the stress tensor, p is the pressure and E is the total energy defined as:

$$E=e(T)+\frac{V\cdot V}{2} \tag{4}$$

e is the internal energy per unit mass. S_r is the radiative heat source. In the present form of the energy equation, reaction source terms are included in S_h, which also contains all other volumetric heat sources, including those form any dispersed phase.

D. Radiative Transfer

In the absence of the radiation-turbulence interaction, one can write the radiative transfer equation (RTE) for a gray absorbing, emitting and scattering medium in the direction s as:

$$\nabla\cdot(I(s)s)=-(\kappa+\sigma_s)I(s)+B(s) \tag{5}$$

Where

$$B(s)=\kappa I_B+\frac{\sigma_s}{4\pi}\int_{4\pi}I(s')\Phi(s',s)d\Omega' \tag{6}$$

Here, $I(s)$ is the radiant intensity in the direction s, κ is the absorption coefficient, σ_s is the scattering coefficient, I_B is the blackbody intensity and Φ is the scattering function. The radiative source term S_r in the (3) is given by:

$$S_r=\kappa\int_{4\pi}[I(s)-I_B]d\Omega \tag{7}$$

In this research, the Rosseland model [12] was used for solving the RTE.

E. Turbulence Modeling

A turbulence model is a computational procedure to close the system of mean flow (1) and (2) and solve them, so that a more or less wide variety of flow problems can be calculated. There are some well known classical turbulence models. In the present work, the standard $k-\varepsilon$ turbulence model [13] was used, which involves solution of the following transport equations for the turbulent kinetic energy k and its dissipation ε.

$$\frac{\partial}{\partial t}(\rho k)+\nabla\cdot(\rho Vk)=\nabla\cdot\left(\frac{(\mu+\mu_t)}{\sigma_k}\nabla k\right)+G_k-\rho\varepsilon \tag{8}$$

$$\frac{\partial}{\partial t}(\rho\varepsilon)+\nabla\cdot(\rho V\varepsilon)=\nabla\cdot\left(\frac{(\mu+\mu_t)}{\sigma_\varepsilon}\nabla\varepsilon\right)+C_{1\varepsilon}\frac{\varepsilon}{k}G_k-C_{2\varepsilon}\rho\frac{\varepsilon^2}{k} \quad (9)$$

Where G_k is the turbulence production term, σ_k and σ_ε are the turbulence Prandtl numbers and $C_{1\varepsilon}$ and $C_{2\varepsilon}$ are model constants.

In order to solve the PDE equations, the second-order schemes and the segregated solution method and the simple pressure velocity coupling algorithm were used. The standard version of the $k-\varepsilon$ model using the following coefficients was employed in the modeling:

$$C_{1\varepsilon}=1.44; C_{2\varepsilon}=1.92; \sigma_k=1; \sigma_\varepsilon=1.314$$

F. NO Models

In this study, two different mechanis have been identified for the formation and destruction of NO, i.e., thermal NO and prompt-NO mechanism:

G. Thermal NO

The formation of thermal NO is determined by the following three extended Zeldovich mechanism:

$$O+N_2 \xleftrightarrow{k_1,k_2} NO+N \quad (10)$$

$$N+O_2 \xleftrightarrow{k_3,k_4} NO+O \quad (11)$$

$$N+OH \xleftrightarrow{k_5,k_6} NO+H \quad (12)$$

Based on the quasi-stead state assumption for N radical concentration, the net rate of NO formation via the foregoing reaction can be determined by:

$$\frac{d[NO]}{dt}=\frac{1}{1+\frac{k_2[NO]}{k_3[O_2]+k_5[OH]}}\times\left[2k_1[O][N_2]-\frac{2k_2}{k_3[O_2]+k_5[OH]}\times\left(k_4[O][NO]+k_6[H][NO]\right)\right] \quad (13)$$

Where

$$k_i=A_iT^{B_i}\exp\left(\frac{-C_i}{T}\right) \quad (14)$$

Where T is temperature, K. The reaction constants, A_i, B_i and C_i, were taken from Baulch et al. [14].

H. Prompt NO

The formation of prompt NO is determined by the following mechanism:

$$CH+N_2 \leftrightarrow HCN+N \quad (15)$$

$$N+O_2 \leftrightarrow NO+O \quad (16)$$

$$HCN+OH \leftrightarrow CN+H_2O \quad (17)$$

$$CN+O_2 \leftrightarrow NO+CO \quad (18)$$

$$NH+H \leftrightarrow N+H_2 \quad (19)$$

$$N+OH \leftrightarrow NO+H \quad (20)$$

For gaseous fuels, the reaction rate for the prompt-NO formation mechanism is given by:

$$\frac{d[NO]}{dt}=k_{pr}[O_2]^b[N_2][Fuel]\exp\left(\frac{-E_a}{RT}\right) \quad (21)$$

Where

$$k_{pr}=1.2\times10^7\left(\frac{RT}{P}\right)^{b+1} \quad (22)$$

$$E_a=60\times10^3\ cal/mol \quad (23)$$

Where T is temperature, K, R is the gas constant, b is related to oxygen mole fraction in the flame and P is the pressure.

III. The Combustion Chamber

In the research, a model of combustion chamber analogue to the power plant's boiler was designed using CFD modeling to examine the NOx emission and formation in the combustion systems and its lowering possibilities. The combustion chamber includes a burner, (an air nozzle and a fuel nozzle) and a stack. The methane is used as the burner fuel.

IV. CFD Modeling

In the present study, the commercial CFD package, FLUENT6.2 was used to model combustion and NOx emission in a combustion chamber in three dimensions. Using this package it will be possible to employ different model of turbulence, radiation, NOx formation and combustion for this modeling. The combustion chamber was divided into almost 400,000 unstructured tetrahedral meshes. The regions close to the burner were meshed into smaller control volumes in order to increase the precision of predictions. Fig. 1 shows the modeled combustion chamber with a burner (an air nozzle and a fuel nozzle).

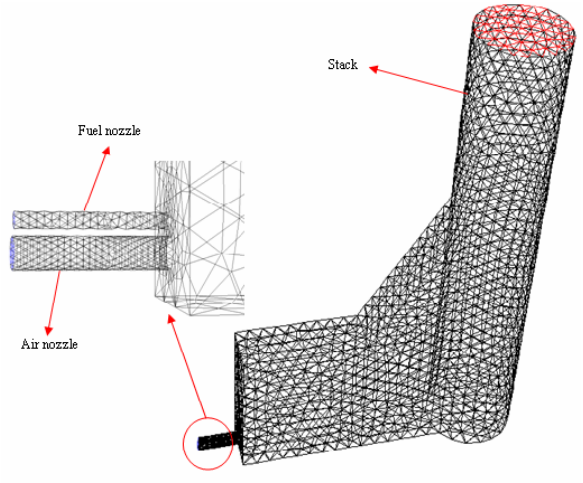

Fig. 1 The modeled combustion chamber with a burner

The governing equations were discretised in the whole volume using the second-order schemes. In addition, the segregated solution method and the simple pressure–velocity coupling algorithm (SIMPLE algorithm) were used to solve the governing equations. The boundary conditions including the fuel flow rate, air flow rate, environment operating condition, etc., were introduced to the model. By converging of the set of PDE equations, the three-dimensional fluid flow parameters, temperature, NOx emission, etc., were obtained.

V. Results and Discussion

The NOx emission is directly proportional to the peak temperature. The peak temperature, in turn, is depended on the preheat air temperature and the oxygen concentration. In order to examine the parameters effects on each other, the combustion was undertaken in different air inlet temperatures ranging between 27-1027°C (300-1300 K) with oxygen different concentrations between 5-23% by weight. During these experiments, the fixed fuel flow rate was considered given that the air flow rate is four times of fuel flow rate. In conventional combustion, the combustion air temperature is 27°C and the oxygen concentration is 23% by weight.

One of the HiTAC features is known as Flameless Oxidation or FLOX. In the flameless oxidation, there is no visible flame in the combustion area. In the present research with respect to the modeling results, observation of the HiTAC combustion in 1027°C combustion air temperature and 5% (mass) oxygen concentration was performed.

Fig. 2 shows the temperature profiles in the conventional combustion and HiTAC. Comparing Fig. 2-a and 2-b shows that in the conventional combustion, the flame has outstanding length and luminosity while in HiTAC, it has low luminosity. Also for conventional combustion, a large variation in the gas temperature is observed while for HiTAC a nearly uniform temperature field is obtained throughout the combustion chamber. In Fig. 2-b there is no visible flame in the combustion chamber, this case is known as flameless oxidation. As the figure shows, in the conventional combustion, the temperature peak is about 1850°C and in HiTAC, it is estimated as 1100°C, so the temperature peak in HiTAC is lower than the conventional combustion.

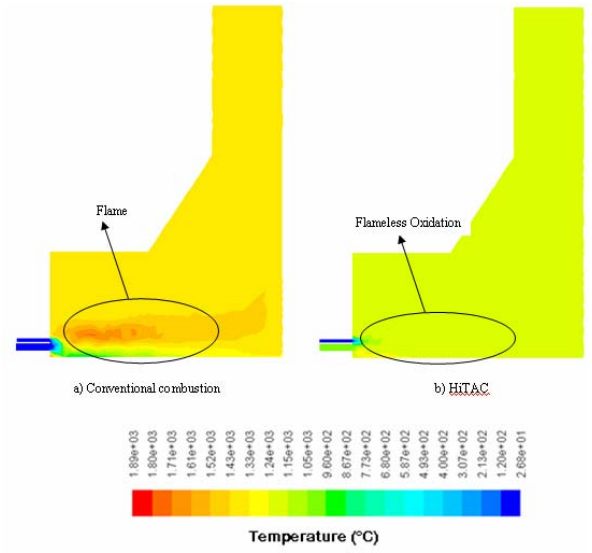

Fig. 2 The temperature profiles in the conventional combustion and HiTAC

Fig. 3 reveals the variations of peak temperature according to various preheat air temperatures in the 23% (mass) oxygen concentration. As the figure shows, the peak temperature would increase with increasing preheat air temperature at a fixed inlet oxygen concentration.

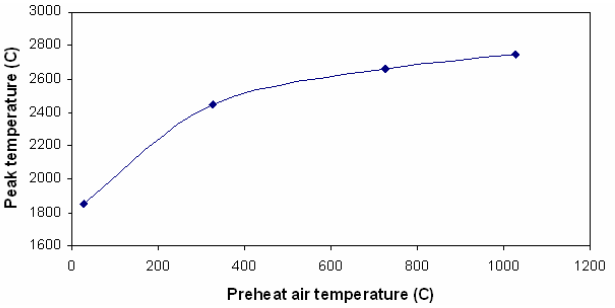

Fig. 3 The variations of peak temperature at a fixed inlet oxygen concentration of 23 % for various inlet preheat air temperatures

Fig. 4 shows the NOx emission levels in the various preheat air temperatures in the 23% (mass) oxygen concentration. As the figure shows, at the fixed oxygen concentration, the increase of preheat air temperature will be associated with the increase of NOx emission. In addition, in the conventional combustion with 27°C preheat air temperature and 23% (mass) oxygen concentration, the NOx concentration is equal to 300 ppm.

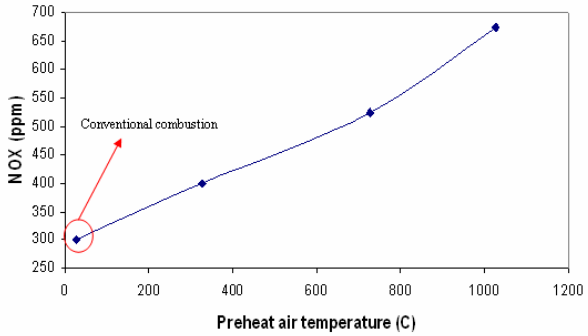

Fig. 4 The NOx emission levels in the various preheat air temperatures in the 23% (mass) oxygen concentration

As it was mentioned, the peak temperature is depended on the preheat air temperature and its oxygen concentration. Fig. 5 demonstrates the variations of peak temperature according to various oxygen concentrations in HiTAC's temperature (1027°C). According to the figure, the peak temperature would decrease with decreasing oxygen concentration at a fixed inlet preheat air temperature.

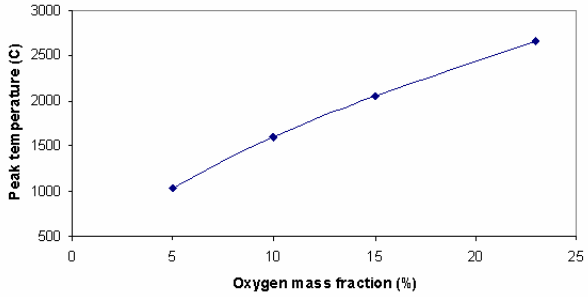

Fig. 5 The variations of peak temperature at various oxygen concentrations in HiTAC's temperature

Fig. 6 shows the NOx emission levels at various oxygen concentrations in 1027°C HiTAC temperature. As it is shown in the figure, given that the preheat air temperature is constant but the oxygen concentration is decreasing, the emission of NOx will also decrease. With respect to the figure, under the HiTAC conditions with 1027°C preheat air temperature and 5 percent oxygen concentration (mass), the NOx concentration is 129 ppm which is less than 133% of conventional combustion.

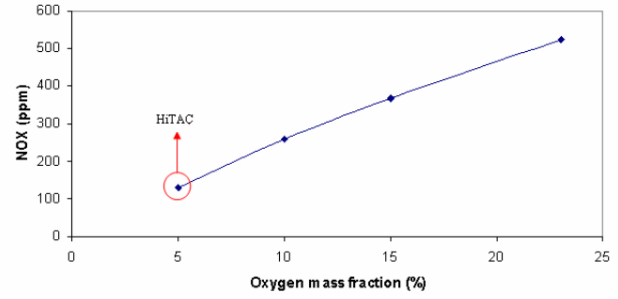

Fig. 6 The NOx emission levels at various oxygen concentrations in HiTAC temperature

Fig. 7 represents the NOx concentration contour plots in the conventional combustion and HiTAC. As Fig. 7-a shows, the NOx emission in the conventional combustion is highest in the flame center because the most important mechanism of NOx emission in the combustion systems is the thermal NOx according which the NOx emission intensity will be very high with the increase of temperature and oxygen concentration. As the highest temperature in the conventional combustion is in the flame center, so the center shows the highest NOx emission rate. In the Fig. 7-b which is related to HiTAC combustion, the lowest NOx emission rate is obtained in the place in which air and fuel are mixed because in the section, the peak temperature and oxygen concentration are relatively low.

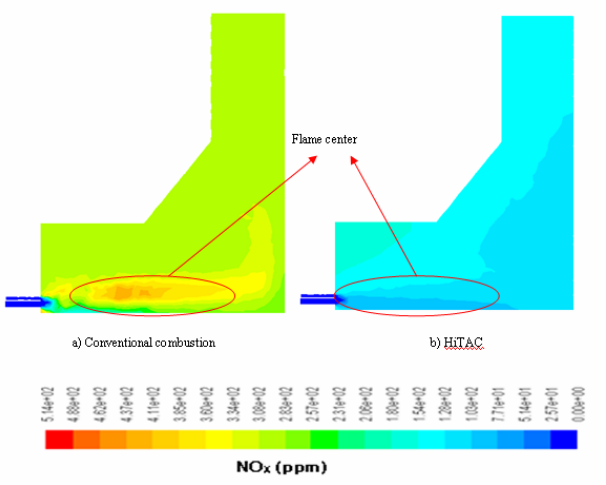

Fig. 7 The NOx concentration contour plots in the conventional combustion and HiTAC

Fig. 8 shows the NOx emission levels as a function of preheat air temperature at 23, 10 and 5% O_2 concentration in air. The emission of NOx increases with preheats air temperature under normal combustion conditions. This was also true for HiTAC conditions but the rate of increase is small. Very low NOx emission is observed under high temperature and low oxygen concentration combustion conditions.

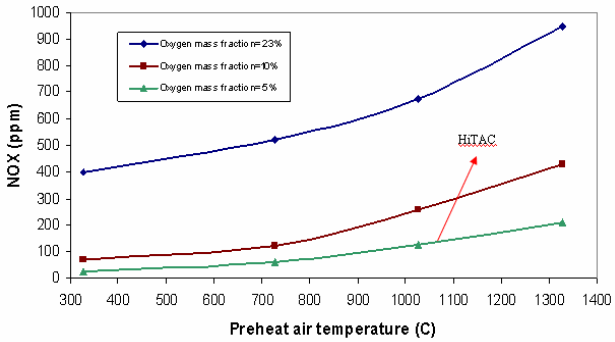

Fig. 8 NOx emission as a function of preheat air temperature and O_2 concentration in air

VI. Conclusion

In the research, the rate of NOx emission as conventional combustion and HiTAC employed in a combustion chamber are examined using CFD modeling. The NOx emission rate is depended on some parameters such as peak temperature, combustion air temperature and oxygen concentration. In this study the effect of these parameters on each other as well as on NOx emission rate was undertaken. Results show that at the fixed oxygen concentration, increasing the preheated air temperature will increase the peak temperature and NOx emission rate. In addition, reduction of the oxygen concentration in a fixed preheated air temperature caused a decreasing trend in the peak temperature and the NOx emission rate. On the other hand, an increase in NOx emission rate was observed with increase of preheated air temperature at various oxygen concentrations. However, the rate of increase in NOx emission using HiTAC technique was significantly lower than that of conventional combustion. The results reveal the importance of CFD for modeling of HiTAC combustion technique.

References

[1] R. Tanaka and T. Hasegawa, "Innovative technology to change flame characteristics with highly preheated air combustion," in 1997 Proc. Japanese Flame Days, Osaka, Japan, pp. 129-150.
[2] A.K. Gupta, "High Temperature Air Combustion: Energy savings, Pollution reduction and Fuel reforming," in Proc. 5th Mediterranean Symposium on Combustion, the Combustion Institute, Monastir, Tunisia, 2007.
[3] S.R. Wu, W.C. Chang and J. Chiao, "Low NOx heavy fuel oil combustion with high temperature air," Fuel, vol. 86, no. 5-6, pp. 820–828, April 2007.
[4] Q. Lu, J. Zhu, T. Niu, G. Song and Y. Na, "Pulverized coal combustion and NOx emissions in high temperature air from circulating fluidized bed," Fuel Process. Technol., vol. 89, no. 11, pp. 1186-1192, Nov. 2008.
[5] S. Li, T. Xu, S. Hui and X. Wei, "NOx emission and thermal efficiency of a 300 MWe utility boiler retrofitted by air staging," Appl. Energ., vol. 86, no. 9, pp. 1797-1803, Sep. 2009.
[6] G. L. Borman and K. W. Ragland, "Combustion Engineering," New York: McGraw-Hill, 1998, pp. 216–221.
[7] A.K. Gupta and Z. Li, "Effect of fuel property on the structure of highly preheated air flames," J. Energ. Resour-ASME, vol. 5, pp. 247-257, June 1997.
[8] T. Hasegawa, S. Mochida and A. Gupta, "Development of advanced industrial furnace using highly preheated combustion air," J. Propul. Power, vol. 18, no. 2, pp. 233-239, Aug. 2002.
[9] A. Kokkinos, D. Wasyluk, D. Adams, R. Yavorsky and M. Brower, "B&W's experience reducing NOx emissions in tangentially-fired boilers," The US EPA/DOE/EPRI combined power plant air pollutant control symposium, the mega symposium, Chicago, Illinois, USA, August 20–23, 2001.
[10] A. Frassoldati, S. Firgerio, E. Colombo, F. Inzoli and T. Faravelli, "Determination of NOx emissions from strong swirling confined flames with an integrated CFD-based procedure," Chem. Eng. Sci., vol. 60. no. 11, pp. 2851–2869, June 2005.
[11] Fluent Inc, Fluent 6.2 User's Guide, 2005.
[12] R. Siegel and J.R. Howell, "Thermal Radiation Heat," Transfer 3rd ed. Hemisphere Publishing Corporation, Washington, 1992.
[13] B.E. Launder and D.B. Spalding, "The numerical computation of turbulent flows," Comp. Meth. Appl. Mech. Eng., vol. 3, no. 2, pp. 269–289, March 1974.
[14] D.L. Baulch, D.D. Drysdall and D.G. Horne, "Evaluated Kinetic Data for High Temperature Reactions," Butterworth, 1973.